Proceedings of the Estonian Academy of Sciences,
2015, **64**, 4, 488–494
doi: 10.3176/proc.2015.4.04
Available online at www.eap.ee/proceedings

MATERIALS SCIENCE

Thermal annealing of sequentially deposited SnS thin films

Maria Safonova[a*], Padmanabhan Pankajakshy Karunakaran Nair[b], Enn Mellikov[a], Rebeca Aragon[b], Karin Kerm[a], Revathi Naidu[a], Valdek Mikli[a], and Olga Volobujeva[a]

[a] Department of Materials Science, Tallinn Technical University, Ehitajate tee 5, 19086 Tallinn, Estonia
[b] Department of Solar Energy Materials, Centro de Investigación en Energía, Universidad Nacional Autónoma de México, Temixco, Morelos 62580, Mexico

Received 16 June 2014, revised 23 April 2015, accepted 14 June 2015, available online 26 November 2015

Abstract. The influence of thermal treatment with the number of deposition cycles on the properties of SnS films on CdS and ZnS substrates was investigated. Annealing under an argon atmosphere made amorphous SnS films formed in one deposition cycle crystalline, but did not markedly change the crystallinity of SnS films formed after multiple deposition cycles. All annealed films were consistent with the orthorhombic phase of herzenbergite SnS, and no additional Sn-containing phases were identified. The CdS/SnS films maintained their initial stoichiometric composition of tin monosulphide after annealing. The films deposited on ZnS substrate films were rich in tin and poor in sulphur and their composition was unaffected by thermal annealing. Both the deposited and thermally annealed films possessed uniform pinhole-free surfaces. Only minor changes in the optical transmittance and reflectance spectra of the CdS/SnS films were observed after annealing, whereas the spectra of the ZnS/SnS films exhibited substantial changes after annealing. As the annealing temperature increased, the absorption edge of the ZnS/SnS films shifted to a longer wavelength. The optical bandgap of the CdS/SnS films was indirect and decreased from 1.28 eV for the three-deposition-cycle CdS/SnS film to 1.22 eV after annealing at 460 °C. The ZnS/SnS films showed a similar change: the bandgap of 1.39 eV for the unannealed films decreased to 1.23 eV after annealing. All deposited and annealed SnS films showed p-type conductivity and their photoconductivity increased with the increasing annealing temperature. Solar cells with reverse structures were fabricated; their performance decreased with the increasing annealing temperature of the SnS film.

Key words: SnS thin films, chemical-bath deposition, X-ray diffraction, optical spectroscopy, atomic force microscopy, scanning electron microscopy.

1. INTRODUCTION

Humankind today is in intensive search for sustainable energy sources. Renewable energy sources such as sun, wind, and water are being examined to increase their proportion in the energy market. Among these, solar radiation has the greatest potential because of its abundance. Materials such as $CuInSe_2$ [1], $CuInS_2$ [2], CdTe [3], and SnS [4] have been used as absorber layers in thin-film solar cells to convert solar radiation to electricity. For this SnS is very promising because of its high absorption coefficient (10^5), suitable bandgap for solar cells, and abundance in nature [5]. SnS thin films have been deposited by techniques such as electrodeposition [6], spray pyrolysis [7], sputtering [8], vacuum evaporation [9], and chemical-bath deposition (CBD) [10–15]. Despite the relatively low cost and simplicity of CBD, research reported on the formation of SnS thin films by CBD is insufficient and the topic needs further investigation.

The focus in this paper is on the CBD of SnS thin films onto different substrates [16] and their subsequent annealing. The novelty of our results lies in the description of the effect of different annealing on the structure, chemical and phase composition, and properties of multiple-cycle deposited and annealed SnS

* Corresponding author, marija.safonova@gmail.com

films. Our results on the influence of substrate material on the chemical and phase compositions and properties of deposited and annealed thin SnS films add new, very valuable information for providing predata to the production of cheap thin-film solar cells used in chemically deposited SnS absorber layers.

2. EXPERIMENTAL

2.1. Deposition of ZnS films

The ZnS thin films were prepared by a CBD technique described elsewhere [17]. Corning glass substrates, which were first washed with a detergent, were placed vertically in a solution and held at room temperature for 24 h. The resulting films were washed, rinsed with deionized water, and then dried. Films were heated in air for 15 min at 270 °C to promote good adherence of the consecutively deposited SnS film.

2.2. Deposition of CdS films

The CdS thin films were prepared by a CBD technique described elsewhere [18]. Corning glass substrates, which were first washed with a detergent and then in an ultrasonic bath with acetone, were placed vertically in a solution for 1.5 h at 80 °C. The resulting films were washed, rinsed with deionized water, and then dried.

2.3. Deposition of SnS films

The SnS thin films were also prepared by the CBD technique. A few drops of hydrochloric acid were added to stannous chloride to dissolve it in order to obtain a molar concentration of 0.03 M of stannous chloride. Tartaric acid was then added to give a molar concentration of 0.44 M. Deionized water and then ammonium hydroxide were added until the pH of the solution was 7. Sodium thiosulphate was added with a molar concentration of 0.03 M. The total volume of the solution was 100 mL. Corning glass substrates with previously deposited CdS or ZnS thin films were placed vertically in this solution at room temperature for 24 h. The obtained films were rinsed with deionized water and then dried. Thicker films were obtained by consecutive deposition for two or three times.

2.4. Thermal annealing

The deposited films were heated under argon for 30 min at 300, 400, or 460 °C in a vacuum oven. The samples were covered with aluminium foil, placed in a Petri dish, and covered again with aluminium foil. The covered samples were placed in the oven and then the chamber was evacuated to about 30 mTorr. Argon was introduced into the chamber to give a pressure of 10 Torr, and the furnace was heated.

2.5. Characterization of films

The crystalline structure of the films was investigated by X-ray diffraction (XRD) analyses with a RigakuUltima IV X-ray diffractometer using Cu Kα radiation with 2θ ranging from 10° to 70°. Raman spectral measurements were made at room temperature on a high-resolution micro-Raman spectrometer (Horiba JobinYvon HR800) equipped with a multichannel CCD detection system in backscattering configuration. An Nd-YAG laser ($\lambda = 532$ nm) with a spot size of 10 μm was used for excitation.

Scanning electron microscope (SEM) (Hitachi SUI 510 and HR-SEM Zeiss ULTRA 55) images were recorded to obtain information about film surface morphology. The elemental composition of the films was determined by energy-dispersive X-ray spectroscopy (EDX; Oxford, x-act). An atomic force microscope (AFM; Bruker Multimode) with a Nanoscope V controller was used to determine the surface roughness of the films. A profilometer (XP Plus Stylus) was used to determine the thickness of the films. The optical transmittance and near-normal specular reflectance of the films were recorded using a scanning spectrophotometer (Shimadzu UV-VIS-NIK) in the wavelength range of 250–2500 nm. Electrical characteristics were measured using an electrometer (Keithley 619) with a programmable voltage source (Keithley 230).

Pairs of three different types of paint electrodes with a size of 5 mm × 5 mm and separation of 5 mm were printed on the surface of the films for the photocurrent measurements. The photocurrent responses of the films were measured under a tungsten halogen lamp providing illumination of 850 W/m^2.

3. RESULTS

3.1. Film thickness

Both series of films (CdS/SnS and ZnS/SnS) decreased in thickness after thermal annealing, which indicates that annealing caused densification of the films. The effect of annealing was more pronounced for films formed by a single deposition cycle compared with those exposed to multiple deposition cycles. For example, the thickness of the one-deposition-cycle CdS/SnS film decreased from 215 to 164 nm upon annealing at 400 °C under Ar for 30 min, whereas the thickness of the two-deposition-cycle CdS/SnS film decreased from 300 to 258 nm after annealing under the same conditions. The thickness of the three-deposition-cycle ZnS/SnS film decreased from 455 to 429 nm after

annealing at 460 °C under Ar for 30 min. This indirectly confirms our conclusion presented in the XRD measurement part that annealing improves the crystallinity of films and makes them denser.

3.2. Structural properties

Figure 1 shows the influence of heat treatment on the crystalline structure of the SnS films deposited on CdS and ZnS substrates. The absence of peaks consistent with the orthorhombic herzenbergite structure of SnS in the XRD patterns of the one-deposition-cycle films indicates that the deposited films are amorphous. The broad peak situated at a small diffraction angle is specific to the amorphous network. However, as the number of deposition cycles increases, the crystallinity of the films improves: the peaks related to SnS become narrower and more intense. The films formed after three deposition cycles exhibit intense, sharp peaks consistent with SnS. Thermal annealing improved the crystallinity of the one-deposition-cycle CBD films, but did not induce any noteworthy changes in the crystallinity of the SnS films formed using multiple deposition cycles. All annealed films clearly show peaks at 31.60°, 26.5°, 22.6°, 38.9°, and 45.3° corresponding to the (040), (120), (110), (131), and (150) planes of the orthorhombic phase of the herzenbergite SnS structure, respectively (see the standard database card 01-072-8499). The existence of CdS with peaks at 26.5°, 30.7°, 51.2°, 53.1°, and 64.1°(standard database cards 04-008-2190 and 04-008-2191) in the XRD patterns of the films containing a CdS underlayer could not be determined precisely because these peaks are very close to those of dominating SnS. No indication of other possible Sn-containing phases in the XRD patterns of the annealed films was found.

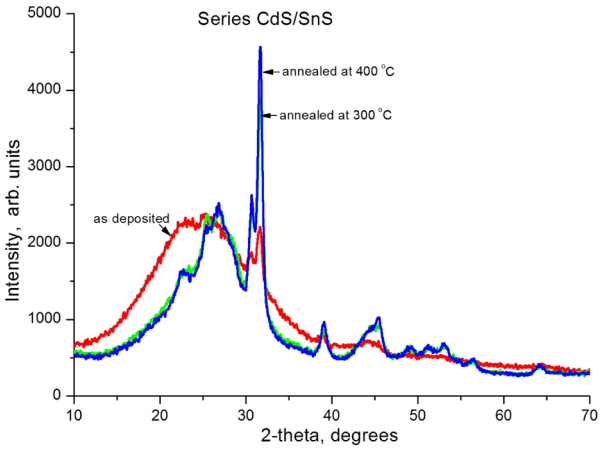

Fig. 1. XRD patterns of CdS/SnS thin films showing the influence of heat treatment on the crystallinity of the two-deposition-cycle SnS deposited films and films annealed at 300 and 400 °C.

The XRD patterns of one-, two-, and three-deposition-cycle SnS films deposited on CdS and ZnS and annealed at 460 °C are compared in Fig. 2. The CdS/SnS films annealed at 460 °C are more crystalline than those deposited on ZnS substrates. All the films exhibit a preferred (040) plane. The peak associated with this plane was used to calculate the crystallite size.

Crystallite size increased with annealing more in films deposited by one deposition cycle than by multiple depositions; for the series annealed at 460 °C from 130 to 163 Å for the one-deposition-cycle CdS/SnS films and from 130 to 143 Å for the three-deposition-cycle ZnS/SnS films.

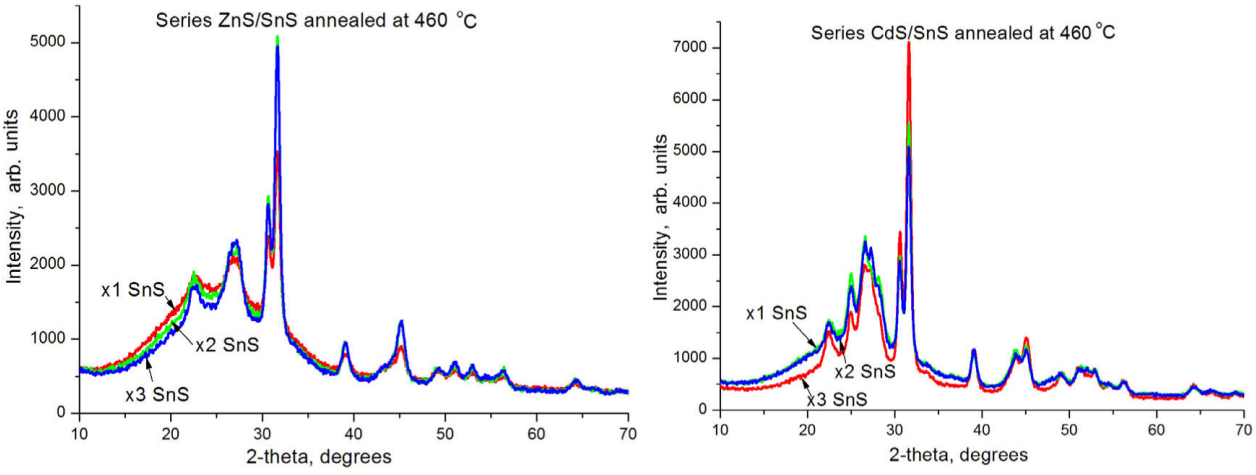

Fig. 2. XRD patterns of ZnS/SnS and CdS/SnS films annealed at 460 °C for 30 min.

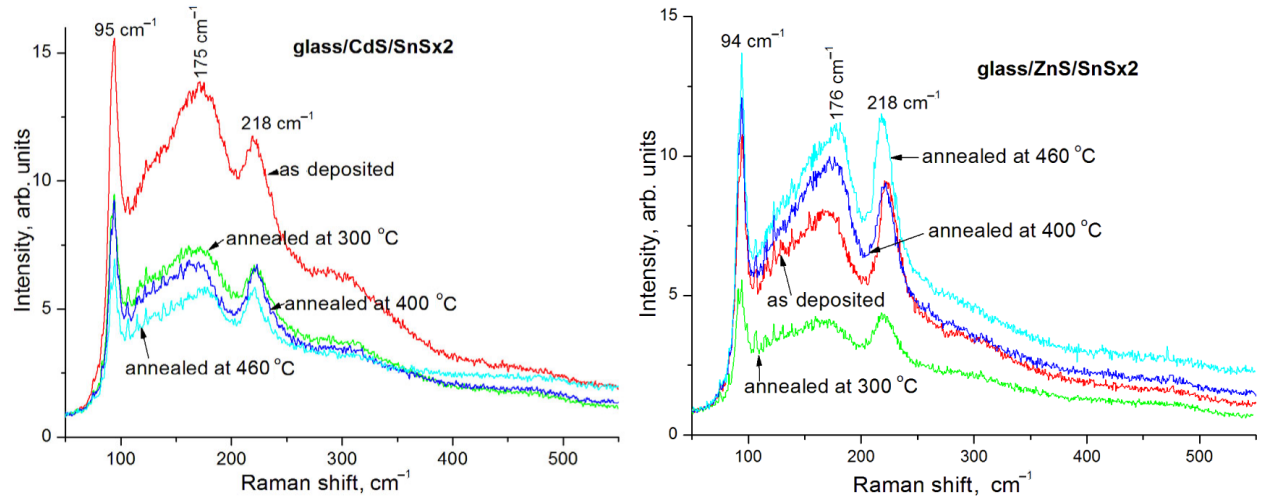

Fig. 3. Raman analyses of two-deposition-cycle films of CdS/SnS and ZnS/SnS annealed at various temperatures.

Results of Raman analyses of the films are presented in Fig. 3. The films show only peaks corresponding to the SnS phase. In the Raman spectrum of the one-deposition-cycle CdS/SnS film, a weak peak at 306 cm^{-1} was detected, which was attributed to CdS (305 cm^{-1}) [19]. This peak could also be attributed to Sn_2S_3 (307 cm^{-1}) [20]; however, other analyses like XRD and EDX showed no presence of any additional SnS phases. This peak disappeared upon thermal annealing. The absence of this peak from the spectra of the ZnS/SnS films (Fig. 3) indirectly supports our assumption that this peak originates in the CdS substrate.

3.3. Elemental analyses and surface morphology

Table 1 shows the atomic ratios of Sn to S in deposited and thermally annealed CdS/SnS and ZnS/SnS films. EDX revealed ratios of Sn to S of almost 1 : 1 in the deposited and annealed films formed on CdS substrates. So annealing did not lead to large changes in the composition of the films; the annealed CdS/SnS films maintained their initial stoichiometric composition of tin monosulphide. Annealing at 460 °C caused the tin composition of films to increase, probably because more sulphur is lost during annealing at higher temperatures. The films deposited on ZnS substrates were rich in tin and poor in sulphur after deposition and their composition remained the same after thermal annealing.

Figures 4 and 5 show SEM images of the CdS/SnS and ZnS/SnS films. Uniform pinhole-free surfaces were observed for both the deposited and thermally annealed

Table 1. Atomic ratios of Sn and S in films of series CdS/SnS and ZnS/SnS

Deposition counts	Series ZnS/SnS		Series CdS/SnS	
	Sn : S Atomic %		Sn : S Atomic %	
Unannealed				
one	50.95	48.04	50.18	49.82
two	53.44	46.56	50.20	49.80
three	56.09	43.60	50.69	49.31
460 °C 30 min				
one	55.46	44.54	51.34	48.66
two	53.02	46.98	51.44	48.56
three	55.17	44.83	52.69	47.31

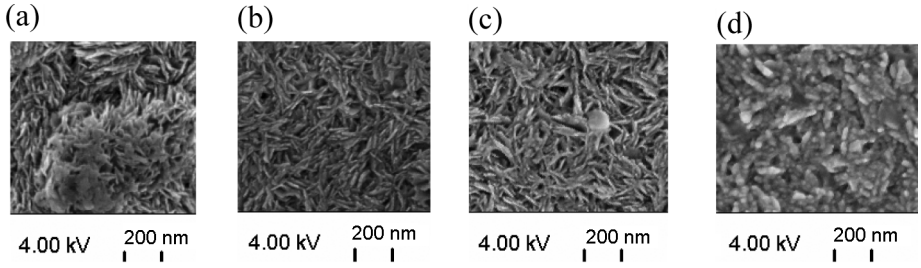

Fig. 4. SEM images of CdS/SnS films formed after two deposition cycles: (a) as deposited, (b) annealed at 300 °C, (c) annealed at 400 °C, and (d) annealed at 460 °C.

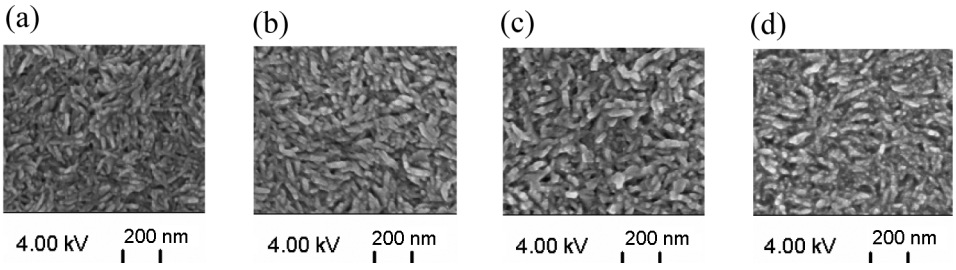

Fig. 5. SEM images of ZnS/SnS films formed after two deposition cycles: (a) as deposited, (b) annealed at 300 °C, (c) annealed at 400 °C, and (d) annealed at 460 °C.

films. Particle size remained nearly the same regardless of the annealing temperature. Films deposited on ZnS substrates have rod-shaped particles, whereas CdS/SnS films contain flake-shaped particles. Annealing at 460 °C changed the surface structure of the films and resulted in films with rod-shaped particles.

3.4. Optical and electrical properties

The optical transmittance (%T) and reflectance (%R) spectra of the CdS/SnS and ZnS/SnS thin films show that the CdS/SnS films exhibit only minor changes in optical transmittance and reflectance after annealing, whereas those of the ZnS/SnS films change markedly. The absorption edge of the ZnS/SnS films shifts to longer wavelengths with increasing annealing temperature. After annealing at 460 °C, the transmittance spectra show bending in the region of 750–900 nm. This could be the reason why the bandgap of these films changed more than that of the CdS/SnS films. However, XRD and Raman data showed no additional SnS phases, so we attribute this bending to defects appearing at the higher annealing temperature. In the present films, the transition was indirect. The energy bandgap (E_g) of the films was determined from the plots of $(\alpha h\nu)^{1/2}$ against photon energy ($h\nu$). The calculated optical bandgaps for the CdS/SnS thin films varied from 1.28 eV for the film formed after three deposition cycles to 1.22 eV after annealing at 460 °C for 30 min under an inert atmosphere. For the ZnS/SnS films, the bandgap of the three-deposition-cycle film was 1.39 eV and decreased to 1.23 eV as the annealing temperature was increased to 460 °C.

The hot-probe method was used to determine the type of conductivity of the films. All deposited and annealed SnS films showed p-type conductivity. All of the films were photosensitive, and their photosensitivity increased with the annealing temperature.

Solar cells were made by depositing a CdS buffer layer onto transparent electrically conductive (TEC) glass substrates and consecutive deposition of SnS films. Different types of electrodes were painted onto the structures to produce solar cells. The best results were obtained using electrodes made of carbon mixed with Se/ZnS powder. Figure 6 presents voltage versus current density curves of solar cells containing SnS deposited on CdS. The performance of the solar cells decreased with the increasing annealing temperature. The best performance was obtained for the unannealed

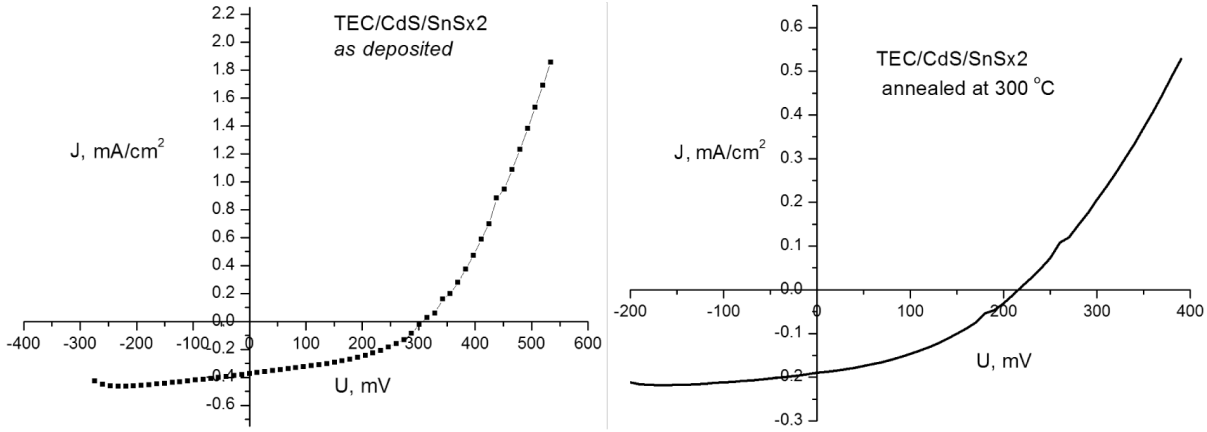

Fig. 6. Voltage–current density curve of a solar cell containing an unannealed SnS film formed after two deposition cycles and annealed at 300 °C.

SnS film formed after two deposition cycles with an open-circuit voltage (Voc) of 0.3 V, short-circuit current density (J_{sc}) of 0.373 mA/cm^2, fill factor of 31.7%, and efficiency of 0.04%.

4. CONCLUSIONS

Our results confirm that after the first deposition cycle, the SnS films are amorphous. As the annealing temperature increases, the films exhibit crystalline structure with preferential orientation. A CdS substrate promotes formation of films with higher crystallinity than a ZnS substrate. The deposited CdS/SnS films had stoichiometric SnS composition, although this was influenced by thermal annealing. A ZnS substrate led to the formation of Sn-rich SnS films with compositions unaltered after thermal annealing. Solar cells containing the films were fabricated; the best results were Voc = 0.3 V and J_{sc} = 0.373 mA/cm^2.

ACKNOWLEDGEMENTS

The authors thank Ana Rosa Garcia for help with experiments, Patricia Altuzar for XRD measurements, Jose Campos for SEM-compositional analyses and photoconductivity response measurements, and Oscar Gomez Daza for optical measurements. All these researchers are based at the Instituto de EnergiasRenovables – UNAM.

The Estonian Centre of Excellence in Research Project TK117T 'High-technology Materials for Sustainable Development', Estonian Energy Technology Program (project AR 10128), Estonian Ministry of Education and Research (targeted project T099), and Estonian Science Foundation (MJD213, G8147) are acknowledged for financial support.

REFERENCES

1. Jeong, S., Lee, B.-S., Ahn, S. J., Yoon, K. H., Seo, Y. H., and Choi, Y. An 8.2% efficient solution-processed $CuInSe_2$ solar cell based on multiphase $CuInSe_2$ nanoparticles. *Energy Environ. Sci.*, 2012, **5**, 7539–7542.
2. Hussain, K. M. A., Podder, J., Saha, D. K., and Ichmura, M. Structural, electrical and optical characterization of $CuInS_2$ thin films deposited by spray pyrolysis. *Indian J. Pure Appl. Phy.*, 2012, **50**, 117–122.
3. Mohammed, W. F., Daoud, O., and Al-Tikriti, M. Power conversion enhancement of CdS/CdTe solar cell interconnected with tunnel diode. *Circuits and Systems*, 2012, **3**, 230–237.
4. Schneikart, A., Schimper, H.-J., Klein, A., and Jaegermann, W. Efficiency limitations of thermally evaporated thin-film SnS solar cells. *J. Phys. D: Appl. Phys.*, 2013, **46**, 305109.
5. Andersson, B. A. Materials availability for large-scale thin-film photovoltaics. *Prog. Photovolt. Res. Appl.*, 2000, **8**, 61–76.
6. Mariappan, R., Ragavendar, M., and Ponnuswamy, V. Structural and optical characterization of SnS thin films by electrodeposition technique. *Opt. Appl.*, 2011, **XLI**, 988–997.
7. Reddy, K. T. R., Reddy, P. P., Miles, R. W., and Datta, P. K. Investigations on SnS films deposited by spray pyrolysis. *Opt. Mater.*, 2001, **17**(1–2), 295–298.
8. Hartman, K., Johnson, J. L., Bertoni, M. I., Recht, D., Aziz, M. J., and Scarpulla, M. A. SnS thin-films by RF sputtering at room temperature. *Thin Solid Films*, 2011, 5**19**, 7421–7424.
9. Ghosh, B., Das, M., Banerjee, P., and Das, S. Fabrication of vacuum-evaporated SnS/CdS heterojunction for PV applications. *Sol. Energ. Mat. Sol. C.*, 2008, **92**, 1099–1104.
10. Sreedevi, G. and Reddy, K. T. R. Properties of tin monosulphide films grown by chemical bath deposition. *Conference Papers in Energy*, 2013, **2013**, Article ID 528724.
11. Ming Du, Xuesong Yin, and Hao Gong. Effects of triethanolamine on the morphology and phase of chemically deposited tin sulfide. *Mater. Lett.*, 2015, **152**, 40–44.
12. Sreedevi Gedi, Vasudeva Reddy Minnam Reddy, Chinho Park, Jeon Chan-Wook, and Ramakrishna Reddy, K. T. Comprehensive optical studies on SnS layers synthesized by chemical bath deposition. *Opt. Mater.*, 2015, **42**, 468–475.
13. Patel, T. H. Influence of deposition time on structural and optical properties of chemically deposited SnS thin films. *The Open Surface Science Journal*, 2012, **4**, 6–13.
14. Ragina, A. J., Preetha, K. C., Murali, K. V., Deepa, K., and Remadevi, T. L. Wet chemical synthesis and characterization of tin sulphide thin films from different host solutions. *Advances in Applied Science Research*, 2011, **2**(3), 438–444.
15. Chao Gao, Honglie Shen, and Lei Sun. Preparation and properties of zinc blende and orthorhombic SnS films by chemical bath deposition. *Appl. Surf. Sci.*, 2011, **257**, 6750–6755.
16. Safonova, M., Nair, P., Mellikov, E., Garcia, A., Kerm, K., Revathi, N., Romann, T., Mikli, V., and Volobujeva, O. Chemical bath deposition of SnS thin films on ZnS and CdS substrates. *J. Mater. Sci.–Mater. El.*, 2014, **25**, 3160.
17. Arenas, O. L., Nair, M. T. S., and Nair, P. K. Chemical bath deposition of ZnS thin films and modification by air annealing. *Semicond. Sci. Tech.*, 1997, **12**, 1323.
18. Nair, P. K., Daza, O. G., Readigos, A. A.-C., Campos, J., and Nair, M. T. S. Formation of conductive CdO layer on CdS thin films during air heating. *Semicond. Sci. Tech.*, 2001, **16**, 651–656.

19. Leite, R. C. C. and Porto, S. P. S. Enhancement of Raman cross section in CdS due to resonant absorption. *Phys. Rev. Lett.*, 1966, **17**, 10.
20. Price, L. S., Parkin, I. P., Hardy, A. M. E., Clark, R. J. H., Hibbert, T. G., and Molloy, K. C. Atmospheric pressure chemical vapor deposition of tin sulfides (SnS, Sn_2S_3, SnS_2) on glass. *Chem. Mater.*, 1999, **11**, 1792–1799.

SnS kilede keemiline sadestamine ZnS ja CdS alusele ning nende järgnev termiline töötlemine

Maria Safonova, Padmanabhan Pankajakshy Karunakaran Nair, Enn Mellikov, Rebeca Aragon, Karin Kerm, Revathi Naidu, Valdek Mikli ja Olga Volobujeva

On uuritud erinevate kasutatavate aluspindade ja Ar atmosfääris läbiviidud termiliste käsitluste mõju keemiliselt sadestatud SnS kilede keemilisele ning faasikoostisele, nende kristallistruktuurile ja optilistele omadustele. On näidatud, et ühekordselt keemiliselt sadestatud SnS kiled on amorfsed. Mitmekordne keemiline sadestus viib ortorombilise kristallistruktuuriga SnS kilede moodustumisele, sõltumata sadestamisel kasutatavast aluspinnast. CdS alusele sadestatud kiled on stöhhiomeetrilise koostisega, mis on muudetav nende kilede järgnevate termiliste käsitlustega. ZnS aluse kasutamine viib Sn-rikaste kilede moodustumisele. Kilede mitteotsese keelutsooni laius E_g on muudetav nende järgnevate termiliste töötlustega. Kolmekordselt sadestatud CdS/SnS kilede keelutsooni laius muutus termilisel käsitlusel temperatuuril 460 °C 1,28 eV-lt kuni 1,22 eV-ni. Analoogselt ZnS/SnS kiledele muutus keelutsooni laius kilede termilistel käsitlustel 1,39 eV-lt kuni 1,23 eV-ni. Keemiliselt sadestatud SnS kilede alusel valmistatud päikesepatarei struktuurid CdS-SnS olid parameetritega Voc = 0,3 V ja J_{sc} = 0,373 mA/cm^2.